

Numerical investigations on the effect of frequency on synthetic jet impingement cooling using multiple orifice

S. Vaishnav

Department of Mechanical Engineering,
TKM College of Engineering (affiliated to APJ Abdul Kalam
Technological University)
Kollam-691005, Kerala, India
vaishnavs240797@gmail.com

R. Leena

Department of Mechanical Engineering,
TKM College of Engineering (affiliated to APJ Abdul Kalam
Technological University)
Kollam-691005, Kerala, India
leenakalidas@gmail.com

Abstract—A synthetic jet generally consists of a cavity with a driver attached on one side and an orifice on the opposite side. When the driver moves back and forth, the jet will generate an unsteady flow through the orifice and the flow will move downstream to a surface forming an impinging flow. When the jet is in the ejection cycle, the diaphragm will expel flow out from the orifice and form a vortex near the orifice. If the propulsion is large enough, the vortex will move downstream before the jet orifice flow reverses and starts to suck in flow. The computational process is carried out using the commercial software ANSYS Fluent. In this study, the heat transfer characteristics of synthetic jet impingement cooling with multiple orifice (1 and 2 orifices) are analyzed with different operating frequencies ($f=100$ Hz to $f=500$ Hz and $f=1$ Hz to $f=5$ Hz) with different Reynolds numbers ($Re=10000$ and 20000). The results demonstrate that high frequency synthetic jets show better heat removal capacity than lower frequency at the same Reynolds number.

Keywords— Synthetic jet, frequency, orifice

I. INTRODUCTION

The Synthetic jets at an aperture use a continuous oscillator, either a piston in a cylinder or a piezoelectric membrane. When used at high enough frequencies, they create a jet pulse that is practically continuous and modifies the working fluid in the surroundings. Large-scale vortices are created by the oscillation of the synthetic jet as opposed to continuous jets, and while no net increase in axial momentum is created, there is no net increase in mass flow rate. Another feature of the flow near the jet's departure is the formation and advection of vortex pairs with stronger entrainment and circulation than continuous jet columns. Synthetic jets are easier to maintain than continuous jets since they operate with surrounding fluid rather than a separate working fluid.

Li *et al.* (2020) numerically analyzed the effect of Strouhal number, frequency (10-75 Hz) as well as Re (10000-20000) on heat transfer behaviors of triangular synthetic jet flow. Using a frequency range of 10-35 Hz, it was observed that the normalized occurrence moment of the highest area-averaged

Nusselt number increasingly lagged at identical Re . Although when frequency is the same, the fluctuation pattern of the area averaged Nusselt number with normalized time is different from that of Re . For each Re , the largest Nusselt number range is a Strouhal number range between 0.24 and 0.48. Due to the great coherence between heat and mass transfer, the individual effects of re and frequency on heat transmission can be connected to their effects on the flow field. These variables lead to variations in flow structure, which affects the features of wall jets, vortex behaviour, and the high-speed zone above the target wall.

Jacob *et al.* (2021) investigated the effect of jet frequency and distance between the orifice and the heated plate. Experimental and numerical techniques were used to evaluate the heat transfer characteristics of synthetic air jets. The results of the investigation show that frequency rises as heat transmission increases. The ideal value of Z/D depends on the jet's frequency. Recirculation and the air entrainment effect that result from low Z/D have an effect on heat transferability. However, at high Z/D ratios and frequencies, this effect is reduced and uniform heat transmission occurs. Synthetic jets have less heat transmission at very low Z/D values because of air recirculation. The heat transfer is strongly impacted by the orifice size for a given frequency.

By adding the fans in the duct, Chaudhari *et al.* (2010) investigated the effectiveness of the synthetic jet impingement in cross flow for heat transfer. The performance of heat transfer was not significantly impacted by the duct's width. The greatest heat transfer coefficient (134 W/m²K) was achieved using a cross flow and synthetic jet combination, which was much greater than cross flow alone but lower than synthetic jet impingement alone.

Chaudhari *et al.* (2011) investigated the impact of various orifices on the enhancement of synthetic jet impingement. A larger circle orifice in the centre and many smaller circular orifices surrounding it were used to measure the satellite orifices' heat transfer coefficients. A 5 mm round hole in the

centre and eight 3 mm round orifices all around it were used to achieve the highest heat transfer coefficient ($159 \text{ W/m}^2\text{k}$). Its value exceeded that of a single round orifice in the centre by 30%. When compared to a single orifice, it was discovered that the heat transfer coefficient for the satellite orifice had two peaks with increasing axial distances.

Mangate *et al.* (2019) studied experimentally the effect of different orifice shapes on the heat transfer of synthetic air jet impingement at different Stokes numbers and pitch ratios. When impinging on a heated surface, the results demonstrate a 75% greater heat dissipation than the single orifice. Only with lower values of pitch ratio were the multiple-orifice designs with one and two satellite orifices able to demonstrate two local maxima in Nu_{avg} . These local peak locations showed little to no Stokes number dependence. In comparison to configurations with a center orifice and the case with a single center aperture, variants without a center orifice showed noticeably less heat transmission. The results further show that, for greater values of pitch ratio ($R \geq 1.25$), the greatest value of Nu_{avg} is located closer to the heated surface and likewise decreases in magnitude.

Kim *et al.* (2021) experimentally studied the flow interaction between two synthetic jets generated from a dual orifice device. They observed that the overall jet merging and combining is enhanced as the orifice spacing and stroke length decrease. The influence of dimensionless orifice spacing and stroke length ($L_0/D = 13.7, 18.6, \text{ and } 27.5$) is analyzed at a fixed Reynolds number of $Re=3700$. The interaction between the two jets is strengthened as the orifice spacing gets smaller, which leads to a quick decay of the centreline velocity of the jet and a rise in the symmetry line velocity, which causes the merging and combining of the jets to happen sooner. Increased stroke length results in lesser entrainment and jet interaction because the leading vortex ring's influence is diminished and the trailing jet's influence is increased. The merging region grows linearly with an increase in stroke length, and the merging point and combined point positions tend to shift downstream as orifice spacing widens. According to a numerical analysis by Jain *et al.* (2011), under similar frequency and amplitude operating conditions, the flow-field of the synthetic jet is more sensitive to changes in orifice dimensions than to those in cavity dimensions. They found that changing the cavity's depth and shape had much less of an impact on the synthetic jet's flow field than changing its orifice size, as long as the amplitude or L remained constant. The radius of the orifice and cavity, as well as the thickness of the orifice plate were shown to be the most important factors. In contrast, according to their experimental work on three holes of the same capacity but with varied shapes.

In order to study the heat transfer properties of jet impingement cooling on a copper disc with a diameter of 12.7 mm and a thickness of 6 mm, Pavlova and Amitay (2006) constructed a synthetic jet using a piezo disc with a diameter of 30.2 mm. It was discovered that lower frequency jets (420 Hz) were more successful at longer axial distances whereas higher frequency jets (1200 Hz) were more effective at smaller axial distances between the orifice plate and the copper disc. At the same Reynolds number, they also

compared synthetic jets to continuous jets and discovered that synthetic jets were three times as effective in cooling. They asserted that this intriguing phenomenon was linked to the buildup of vortex using Particle Image Velocimetry.

The characteristic of the local Nusselt number is compared to the work of Cadek and Gardon and Akfirat (1966) in order to further validate. For the grid independence study, the grid sizes of 351×171 , 381×191 , and 401×201 are taken into consideration. The grid independence research, shown in Figure (4), plots non-dimensional variation of wall shear stress for grid sizes 351×171 , 381×191 , and 401×201 . Nonetheless, to be on the safe side, a grid size of 381×191 is chosen for the current computation despite the fact that the change of non-dimensional wall shear stress with three grid levels is relatively modest.

Manca *et al.* (2011) studied on confined impinging slot jet working with a mixture of water and Al_2O_3 nanoparticles. In order to study the behaviour of the system in terms of average and local Nusselt numbers, convective heat transfer coefficient and necessary pumping power profiles, temperature fields, and stream function contours, various geometric ratios, particle volume concentrations, and Reynolds numbers have been taken into consideration. The dimensionless stream function contours demonstrate how the confining effects, as shown by the H/W ratio, Reynolds number, and particle concentrations, affect the size and intensity of the vortex forms. The local Nusselt number profiles exhibit maximum values at the stagnation point and minimum values near the heated plate's edge. The average Nusselt number rises with increasing particle concentrations and Reynolds numbers. In addition, the highest values are seen for $H/W = 10$, and a maximum increase of 18% is found at a concentration of 6%.

A synthetic jet ejector heat sink was created by Mahalingam (2007), Mahalingam *et al.* (2004) and Mahalingam and Glezer (2005) and its thermal performance was evaluated. By including the synthetic jet, the heat sink's thermal resistance can be decreased from $3.15 \text{ }^\circ\text{C/W}$ to $0.76 \text{ }^\circ\text{C/W}$. It was discovered that the heat sink could dissipate 59.2 W of heater power with a temperature difference of under $70 \text{ }^\circ\text{C}$. In comparison to steady flow in the channel, the heat sink with a synthetic jet was shown to dissipate around 40% more heat.

Li *et al.* (2019) numerically investigated Heat transfer and flow structure of Al_2O_3 - H_2O nanofluids periodic pulsating slot-jet impingement with rectangular wave (R-Wave) and triangular wave (T-Wave). T-wave is better than R-wave at enhancing heat transfer through volume fraction and Re for zero-net-mass flow pulsating jets, especially at higher frequencies (f). Volume fraction and Re both rise with an increase in the average Nusselt number, and they also demonstrate a positive reciprocal promotion relationship that improves heat transmission. The frequency-induced trend reveals a nonlinear trend in which the effect of f on the enhancement of heat transfer is weaker at higher frequencies. The increment rate of average Nusselt number is lowered up to $f=20 \text{ Hz}$. It will be more steady and effective at $f=20 \text{ Hz}$ than $f=50 \text{ Hz}$ at higher Re .

The effects of the Strouhal numbers (0.011, 0.022, and 0.044) and orifice to plate distances (2, 4 and 6 orifice diameters) on the flow field of an impinging zero-net-mass-flux jet at a Reynolds number of 35000 were experimentally investigated by Liu *et al.* (2019). Because it controls how the vortex ring and the following jet have an impact on the flow field, the Strouhal number primarily influences the ZNMF jet structure. When Strouhal numbers are high, the vortex ring is what most distinguishes the flow field. This vortex ring causes a faster flow rate and entrainment, which causes the jet to widen and slow down near its centre. With this Strouhal number, the reduced extent of the following jet results in a smaller extension of the potential core, a greater centerline turbulent kinetic energy, and a closer starting point for the high turbulence level. A lower centerline phase-correlated kinetic energy and a shorter saddle point excursion result from a reduced stroke length, which is implied by a high Strouhal number. Because the tail jet is the most significant component of the flow field at low Strouhal numbers, the behavior entirely changes.

The cooling capabilities of artificial jets were quantitatively studied by Liu *et al.* (2019). Analysis is done on the impact of nozzle to surface distance on cooling performance. The findings demonstrate that when the distance between the nozzle and the surface increases, the cooling ability of synthetic jets initially rises and then falls.

II. PRINCIPLE OF SYNTHETIC JET

A synthetic jet generally consists of a cavity with a driver attached to one side and an orifice on the opposite side. When the driver moves back and forth, the jet will generate an unsteady flow through the orifice and the flow will move downstream to a surface forming an impinging flow. When the jet is in the ejection cycle, the diaphragm will expel flow out from the orifice and form a vortex near the orifice. If the propulsion is large enough, the vortex will move downstream before the jet orifice flow reverses and starts to suck in flow. Synthetic jet impingent is another innovative method for active cooling. In a simple structure and with a low power requirement, the synthetic jet can produce unsteady, turbulent impinging flow. A synthetic jet is a zero-net mass-flux device widely used in boundary-layer separation control, jet vectoring, mixing enhancement in combustion, and turbulence generation (Figure 1).

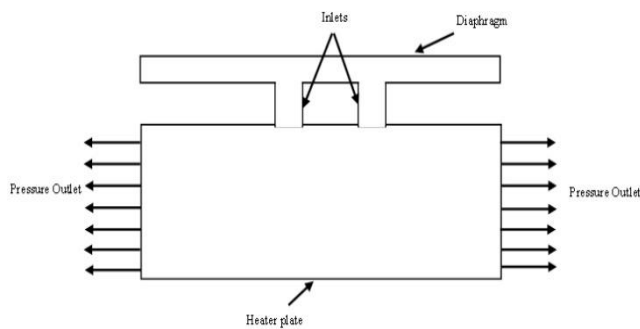


Fig 1: Operation principle of Synthetic-Jet

A. Method for Numerical Simulation

Governing equations

The heat and mass transfer process of synthetic jet is assumed as unsteady, two-dimensional, incompressible, turbulent as well as possessing constant physical properties. Based on those simplifications above, the governing equations in terms of RANS (Reynolds Averaged Navier –Stokes) of this work are written as,

$$\frac{\partial u_i}{\partial x_i} = 0 \quad (1)$$

$$\rho \left(\frac{\partial u_i}{\partial t} + \frac{\partial u_i u_j}{\partial x_j} \right) = - \frac{\partial p}{\partial x_i} + \frac{\partial}{\partial x_i} \left[\mu \left(\frac{\partial u_i}{\partial x_j} + \frac{\partial u_j}{\partial x_i} \right) - \rho u_i' u_j' \right] \quad (2)$$

$$\frac{\partial T}{\partial t} + u_j \frac{\partial T}{\partial x_j} = \alpha \frac{\partial}{\partial x_j} \frac{\partial T}{\partial x_j} - \frac{\partial u_j' T'}{\partial x_j} \quad (3)$$

where the term of $-\rho u_i' u_j'$ represents the Reynolds stresses.

Boundary conditions and turbulence model

The flow is assumed to be three-dimensional incompressible and turbulent. The effect of temperature on the properties of the fluid such as density, viscosity, and thermal conductivity is considered. The turbulent model used is SST k- ω turbulent model. In the case of impinging the target surface, the effects in the near-wall region should be taken into account while the k- ω model specializes in the aspect. Moreover, to make a trade-off between computational efficiency and accuracy, the shear stress transport k- ω (SST/ k- ω) model is employed.

- Inlet condition: velocity inlet UDF
- Wall condition: no slip wall with constant heat flux of 4000W/m² given at the bottom of the plate.
- Outlet condition: Pressure outlet
- Target plate: Copper (Size- 130 x 130 x 24 (mm))
- Cooling medium: Air

Velocity inlet boundary condition is applied at the jet inlet as described,

$$U = U_{max} \sin(2\pi ft) \quad (4)$$

Where U_{max} is the maximum velocity/amplitude, f is the frequency of oscillation and t is the time. A User Defined Function (UDF) is written for the periodic velocity and applied at the oscillating location. Figure 3 shows circular orifice plates of different diameters and the mesh domain of a plate with 16 orifices.

Calculation of Non-dimensional parameters

The Reynolds number is defined as the following Equation (5)

$$Re = \frac{\rho U_0 D}{\mu} \quad (5)$$

Where,

ρ - density of fluid, kg/m³

U_0 – velocity of fluid, m/s

D – Hydraulic diameter of orifice, m μ - Dynamic viscosity of fluid, kg/ms

The Nusselt number is defined as

$$Nu(x,t) = hD/k \quad (6)$$

h-heat transfer coefficient, W/m²K D-the diameter of the orifice,m

k is the thermal conductivity of the fluid, W/mK.

The average velocity presented in Equation (7),

$$U_0 = f \cdot \int_0^T u(t) dt = \frac{1}{T} \cdot \int_0^T u(t) dt \quad (7)$$

where T symbolizes the whole period whereas the integral interval is only the ejection phase; the integral is defined as

Time-area averaged Nusselt number Nu_{avg} , which is defined as the form in Equation (8), is used to estimate the mean heat transfer effect among the whole heated region.

$$Nu_{avg} = \frac{1}{\Delta t} \frac{1}{\Delta x} \int_0^T \int_0^{L/2} Nu(x,t) dx dt \quad (8)$$

where L stands for the length of whole target wall; L /2 represents the length of heated region.

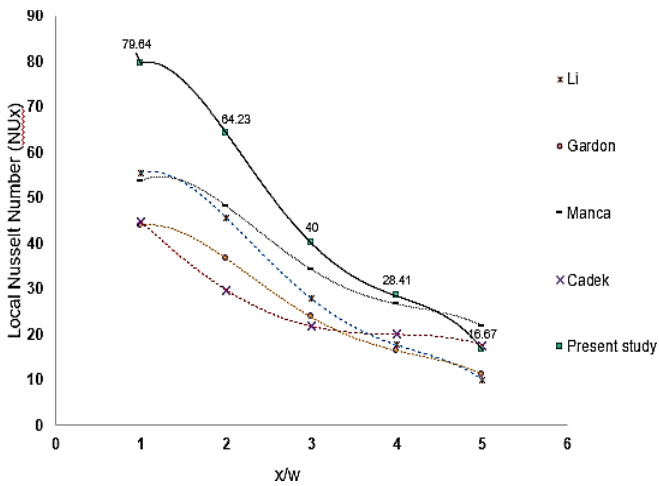
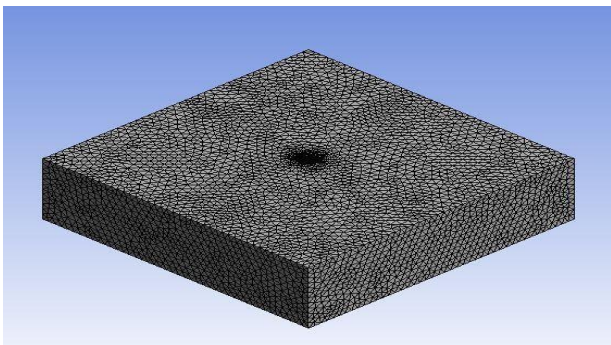


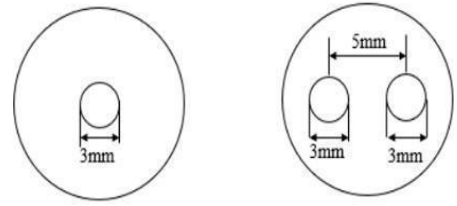
Fig 2: Comparisons of local Nusselt number in present model with reference.

Similarly, the area-averaged Nusselt number Nu_A is given in Eq. (9)

$$Nu_A(t) = \frac{1}{\Delta x} \int_0^{L/2} Nu(x,t) dx \quad (9)$$



(a)



(b)

Fig 3: (a) Mesh domain for single orifice and (b) arrangement of 2 orifices

Numerical Analysis

Numerical studies have been carried out to understand the unsteady behavior of synthetic jets, using the commercial software ANSYS Fluent. The oscillating diaphragm was defined as a moving wall with a turbulence model of shear stress transport (SST) k- ω model. In the case of synthetic jet, k- ω model taken into account to find the effects in the near wall region.

Grid independent study is done to obtain the optimum number of elements. In Figure 4, by comparing the mesh configurations, after 109688 elements the variation of the average Nusselt number is relatively less for Re=10000, Z/d =8mm. The time step number of 100 in one period is regarded as adequate after evaluation.

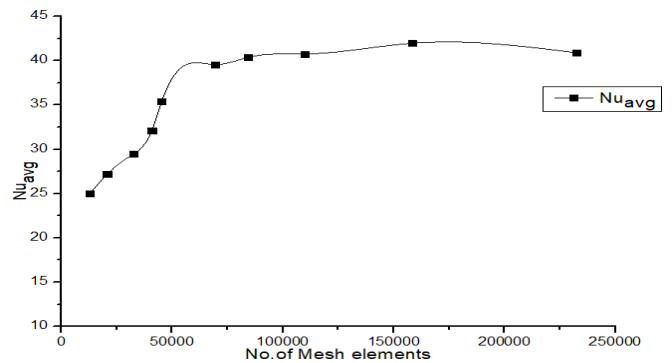


Fig 4: Grid independent study

Table 1: Ranges of Studied Parameters

Parameters	Value
Frequency, f (Hz)	1, 2, 3, 4, 5, 100, 200, 300, 400, 500
Reynolds number, Re	10000, 20000

III. RESULTS AND DISCUSSIONS

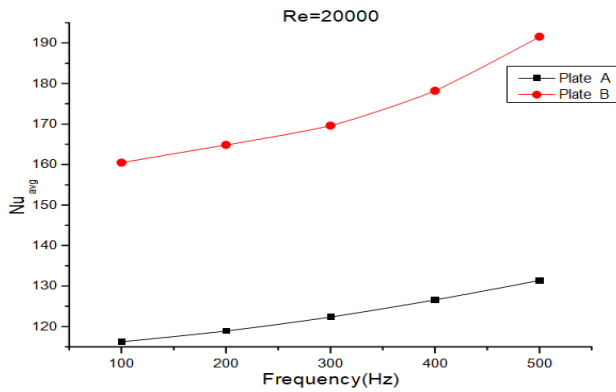
A. Validation

The numerical scheme is validated with the numerical investigations by Manca *et al.* (2011) and experimental study provided by Gardon and Akfirat (1966) as well as Cadek (1968) in the same condition of $Re=11000$, $Z/d=6$.

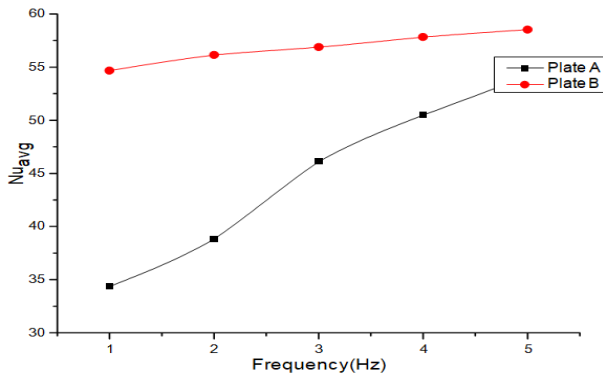
The results are shown in Figure 2. The current results are in great consistency and also exhibit approximate value in the experimental results with those of literatures close to the stagnation point. There is a 15% variation between the present model and reference. Therefore, the proposed model in present work is regarded as reliable judging from the comparison results, and further numerical analyses are to be conducted based on this validated model.

B. Effect of high and low frequencies on average Nusselt number

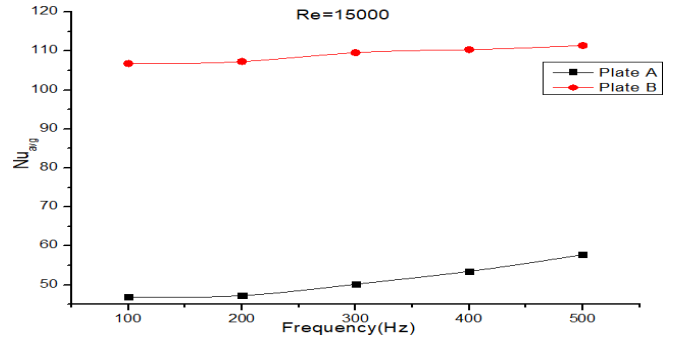
The frequencies vary from 1 Hz to 5 Hz in the range of 1 Hz and from 100 Hz to 500 Hz in the range of 100 Hz. For all these frequencies, studies have been conducted by varying the Reynolds number from 10000 to 20000 in the range of 5000. Figure 5(a) and (b) show the variation of the average Nusselt number for a $Re=20000$. As the frequency increases average Nusselt number also increases for the frequency range of 100 Hz to 500 Hz in the range of 100 Hz.



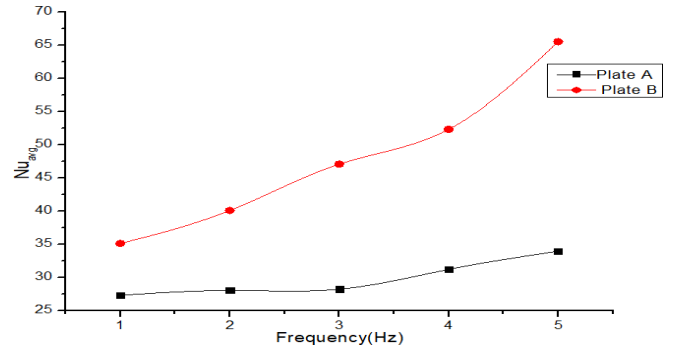
(a)



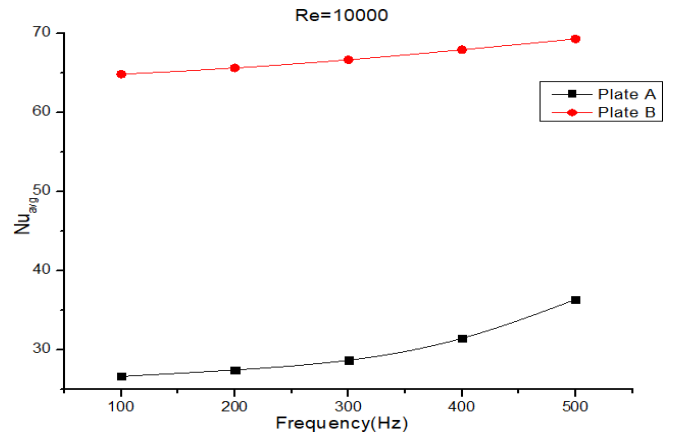
(b)



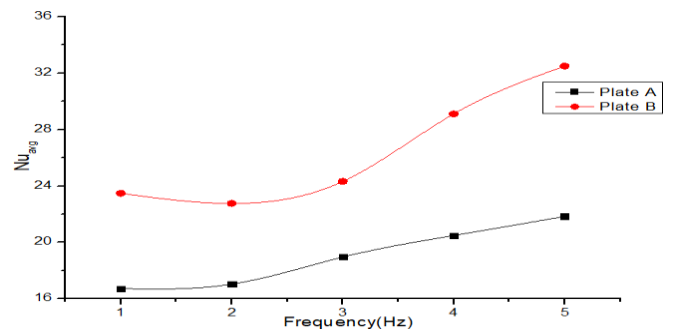
(c)



(d)



(e)



(f)

Fig 5: Effect of high and low frequencies on average Nusselt number at (a) $Re=20000$, (b) $Re=20000$, (c) $Re=15000$, (d) $Re=15000$, (e) $Re=10000$ and (f) $Re=10000$

A large increase in variation can be seen for Plate A at low frequencies (1 to 5 Hz). A similar trend is noted for Plate B shown in Figure 5(b). The same trend lines are formed in the case of $Re=15000$ and $Re=10000$ at high frequencies from 100Hz to 500Hz which are shown in graphs Figure 5(c) and Figure 5(e). But for low frequencies the variation of single orifice is low i.e. the heat transfer rate is very low. But for 2 orifices, the outcome of the value of average Nusselt number is very high i.e., the number of orifices increase the heat transfer rate. The variation of low frequencies for $Re=15000$ and $Re=10000$ are shown in Figure 5(d) and Figure 5(f). At low Reynolds numbers, the synthetic jet flow is laminar and has a low momentum transfer, resulting in a weak cooling effect. As the Reynolds number increases, the synthetic jet flow becomes turbulent, which enhances the mixing of the fluid and leads to a stronger cooling effect. However, at high Reynolds numbers, the synthetic jet flow can become unsteady, which may decrease the cooling effectiveness due to the fluctuation of the impinging jet.

IV. CONCLUSION

A numerical investigation was carried out to study the effects of frequency, Reynolds number, and number of orifices on the heat transfer characteristics of synthetic jet cooling. The analysis is done with a single orifice and 2 orifice plates with different operating frequencies ($f=1$ Hz to $f=5$ Hz and $f=100$ Hz to $f=500$ Hz) with different Reynolds numbers ($Re=10000$ to 20000). The results indicate that as the frequency increases, the average Nusselt number increases for all plates with increase in the number of orifices. Multiple orifice exhibits higher heat transfer rate as compared to single orifice with same the diameter. The effect of high and low frequencies on the average Nusselt number in synthetic jet impingement cooling is dependent on the specific application and desired cooling performance. Low frequencies can enhance heat transfer by promoting large-scale vortex structures that increase the average Nusselt number and improve cooling performance. An increase in Reynolds number leads to an increase in heat transfer due to the enhanced fluid mixing and turbulence induced by the synthetic jet flow. The number of orifices in synthetic jet cooling affects the heat transfer performance by influencing the flow structure, momentum transfer, and pressure drop. Increasing the number of orifices generally leads to a higher heat transfer coefficient, but it can also increase the pressure drop and pumping power requirements. Therefore, the optimal number of orifices needs to be determined based on the specific application and operating conditions.

REFERENCES

[1] Cadek, F. F. (1968). A Fundamental Investigation of Jet Impingement Heat Transfer. Doctoral Dissertation, University of Cincinnati.
[2] Chaudhari, M., Puranik, B., & Agrawal, A. (2010). Heat Transfer Analysis in a Rectangular Duct Without and With Cross-Flow and an Impinging Synthetic Jet. *IEEE Transactions on Components and Packaging Technologies*, 33(2), 488-497. <https://doi.org/10.1109/TCAPT.2010.2042716>

[3] Chaudhari, M., Puranik, B., & Agrawal, A. (2011). Multiple orifice synthetic jet for improvement in impingement heat transfer. *International Journal of Heat and Mass Transfer*, 54(9-10), 2056-2065. <https://doi.org/10.1016/j.ijheatmasstransfer.2010.12.023>
[4] Gardon, R., & Akfirat, J. C. (1966). Heat Transfer Characteristics of Impinging Two-Dimensional Air Jets. *ASME Journal of Heat and Mass Transfer*, 88(1), 101-107. <https://doi.org/10.1115/1.3691449>
[5] Jacob, A., Shafi, K. A., & Roy, K. E. R. (2021). Heat transfer characteristics of piston-driven synthetic jet. *International Journal of Thermofluids*, 11, 100104. <https://doi.org/10.1016/j.ijft.2021.100104>
[6] Jain, M., Puranik, B., & Agrawal, A. (2011). A numerical investigation of effects of cavity and orifice parameters on the characteristics of a synthetic jet flow. *Sensors and Actuators A: Physical*, 165(2), 351-366. <https://doi.org/10.1016/j.sna.2010.11.001>
[7] Kim, M., Lee, H., & Hwang, W. (2021). Experimental study on the flow interaction between two synthetic jets emanating from a dual round orifice. *Experimental Thermal and Fluid Science*, 126, 110400. <https://doi.org/10.1016/j.exptthermflusci.2021.110400>
[8] Li, P., Guo, D., & Liu, R. (2019). Mechanism analysis of heat transfer and flow structure of periodic pulsating nanofluids slot-jet impingement with different waveforms. *Applied Thermal Engineering*, 152, 937-945. <https://doi.org/10.1016/j.applthermaleng.2019.01.086>
[9] Li, P., Huang, X., & Guo, D. (2020). Numerical analysis of dominant parameters in synthetic impinging jet heat transfer process. *International Journal of Heat and Mass Transfer*, 150, 119280. <https://doi.org/10.1016/j.ijheatmasstransfer.2019.119280>
[10] Liu, Z., Yu, Q., Mei, Z., & Xie, D. (2019). Impingement Cooling Performance Analysis and Improvement of Synthetic Jets for Electronic Devices. *Journal of Thermophysics and Heat Transfer*, 33(3), 856-864. <https://doi.org/10.2514/1.T5723>
[11] Mahalingam, R. (2007). Modeling of Synthetic Jet Ejectors for Electronics Cooling. Twenty-Third Annual IEEE Semiconductor Thermal Measurement and Management Symposium (pp. 196-199). IEEE. <https://doi.org/10.1109/STHERM.2007.352423>
[12] Mahalingam, R., & Glezer, A. (2005). Design and Thermal Characteristics of a Synthetic Jet Ejector Heat Sink. *Journal of Electronic Packaging*, 127(2), 172-177. <https://doi.org/10.1115/1.1869509>
[13] Mahalingam, R., Rumigny, N., & Glezer, A. (2004). Thermal management using synthetic jet ejectors. *IEEE Transactions on Components and Packaging Technologies*, 27(3), 439-444. <https://doi.org/10.1109/TCAPT.2004.831757>
[14] Manca, O., Mesolella, P., Nardini, S., & Ricci, D. (2011). Numerical study of a confined slot impinging jet with nanofluids. *Nanoscale Research Letters*, 6, 188. <https://doi.org/10.1186/1556-276X-6-188>
[15] Mangate, L., Yadav, H., Agrawal, A., & Chaudhari, M. (2019). Experimental investigation on thermal and flow characteristics of synthetic jet with multiple-orifice of different shapes. *International Journal of Thermal Sciences*, 140, 344-357. <https://doi.org/10.1016/j.ijthermalsci.2019.02.036>
[16] Pavlova, A., & Amitay, M. (2006). Electronic Cooling Using Synthetic Jet Impingement. *ASME Journal of Heat and Mass Transfer*, 128(9), 897-907. <https://doi.org/10.1115/1.2241889>